HEALTH AND MEDICINE

Pretargeted delivery of PI3K/mTOR small-molecule inhibitor–loaded nanoparticles for treatment of non-Hodgkin's lymphoma

Kin Man Au[1,2], Andrew Z. Wang[1,2]*, Steven I. Park[3,4]*

Overactivation of the PI3K/mTOR signaling has been identified in non-Hodgkin's lymphoma. BEZ235 is an effective dual PI3K/mTOR inhibitor, but it was withdrawn from early-phase clinical trials owing to poor solubility and on-target/off-tumor toxicity. Here, we developed a nanoparticle (NP)–based pretargeted system for the therapeutic delivery of BEZ235 to CD20- and HLA-DR–expressing lymphoma cells for targeted therapy. The pretargeted system is composed of dibenzocyclooctyne-functionalized anti-CD20 and anti-Lym1 antibodies as the tumor-targeting components and azide-functionalized BEZ235-encapsulated NPs as the effector drug carrier. Using lymphoma cell lines with different CD20 and HLA-DR antigen densities as examples, we demonstrate that the dual antibody pretargeted strategy effectively raises the number of NPs retained on the target tumor cells and improves the in vitro and in vivo antitumor activity of BEZ235 through the inhibition of the PI3K/mTOR pathway. Our data demonstrate that the NP-based pretargeted system improves the therapeutic window of small-molecule kinase inhibitor.

INTRODUCTION

Non-Hodgkin's lymphoma (NHL) is one of the most common types of hematologic malignancies in the United States (*1*). In 2018, 75,000 Americans were newly diagnosed with NHL, and an estimated 20,000 died from it (*1*). Anti-CD20 (α-CD20) monoclonal antibodies (Abs), such as rituximab, have revolutionized the treatment of NHL, but 35 to 40% of patients with NHL still relapse after rituximab-containing therapy, such as R-CHOP (rituximab, cyclophosphamide, doxorubicin, and prednisone) (*2*, *3*). Some data indicate that low antigen density, antigen shedding, and/or internalization of CD20 antigens in malignant lymphoma cells could be responsible for resistance to rituximab (*4*–*6*). For this reason, Abs that target other common lymphoma markers [e.g., CD19 (*7*), CD22 (*8*), and HLA-DR (*9*)] have been investigated. In addition, Ab-drug conjugates (*10*) have been developed as second-line treatments for relapsed NHL. Although promising, these functionalized Abs are limited by low drug loading (*11*, *12*), and they are often affected by off-tumor side effects due to potent toxicity of the conjugated drugs (*13*). Novel treatment strategies are needed to improve the therapeutic window of the effector molecule. Recent advances in bioorthogonal click chemistry have facilitated the development of new pretargeted drug delivery systems (*14*, *15*).

The B cell receptor (BCR) pathway plays a key role in the control of cellular proliferation, survival, differentiation, and migration of normal and malignant B cells (*16*–*18*). Thus, interfering with BCR signaling is a rational approach to the treatment of B cell malignancies (*16*–*18*). The phosphatidylinositol 3-kinase (PI3K)/mammalian target of the rapamycin (mTOR) signaling pathway is a key intercellular signal transduction cascade in the BCR pathway (*19*, *20*). Overactivation of PI3K signaling has been identified in multiple malignancies, including NHL (*21*, *22*). PI3K has four main isoforms, which include α, β, γ, and δ (*19*, *20*, *23*). The overexpression of PI3K-α links to the immune escape mechanism, while PI3K-δ is only expressed in hematopoietic cells and plays a key role in B cell proliferation and function (*23*). In vitro study (*24*) and clinical trial (*25*) have demonstrated that inhibition of PI3K can additively or synthetically inhibit the BCR pathway with α-CD20 Abs. BEZ235 is a dual pan-class I PI3K- and mTOR-targeted agent with inhibitory activities predominantly against the α, γ, and δ isoforms of PI3K and mTOR [half-maximal inhibitory concentrations (IC_{50}s) < 10 nM] (*26*, *27*). BEZ235 showed promising in vitro antitumor activities (*26*, *27*), but on the basis of its poor water solubility, BEZ235 must be administered orally in a polyethylene glycol (PEG)–based formulation in humans (*28*, *29*). Furthermore, phase 1/2 clinical trials revealed that the orally administered BEZ235 has poor bioavailability, limited antitumor activities, and high gastrointestinal toxicity (*28*, *29*). Thus, BEZ235 was withdrawn from further trials (*28*, *29*), although several new formulations have recently been reported for topical delivery of BEZ235 (*30*, *31*).

In this research article, we report a two-step dual Ab pretargeted nanoparticle (NP) system for the delivery of BEZ235 to tumor cells as an effective therapy against B cell lymphoma. The system is composed of dibenzocyclooctyne (DBCO)–functionalized α-CD20 [α-CD20(D)] and α-Lym1 [α-Lym1(D)] Abs as the tumor-targeting component and azide-functionalized BEZ235-load poly(ethylene glycerol)-block-poly(lactide-co-glycolide) (PEG-PLGA) NPs (BEZ235 NPs) as the therapeutic effector. Using four established lymphoma cells with different CD20 and HLA-DR antigen densities as examples (fig. S1), we demonstrate that the bioorthogonal pretargeted strategy effectively increases the amount of azide-functionalized therapeutic effector retained on the surface of lymphoma cells, hence enhancing the in vitro antitumor activities of BEZ235 NPs versus free BEZ235 (Fig. 1A). Comprehensive in vivo antitumor efficacy and mechanistic studies using Namalwa and Raji tumor models confirm that the dual

[1]Laboratory of Nano- and Translational Medicine, Carolina Center for Cancer Nanotechnology Excellence, Carolina Institute of Nanomedicine, University of North Carolina at Chapel Hill, Chapel Hill, NC 27599, USA. [2]Department of Radiation Oncology, Lineberger Comprehensive Cancer Center, University of North Carolina at Chapel Hill, Chapel Hill, NC 27599, USA. [3]Lineberger Comprehensive Cancer Center, University of North Carolina at Chapel Hill, Chapel Hill, NC 27599, USA. [4]Levine Cancer Institute, Atrium Health, Division of Hematology and Oncology, 1021 Morehead Medical Dr, Suite 20121, Charlotte, NC 28025, USA.
*Corresponding author. Email: zawang@med.unc.edu (A.Z.W.); steven.park@atriumhealth.org (S.I.P.)

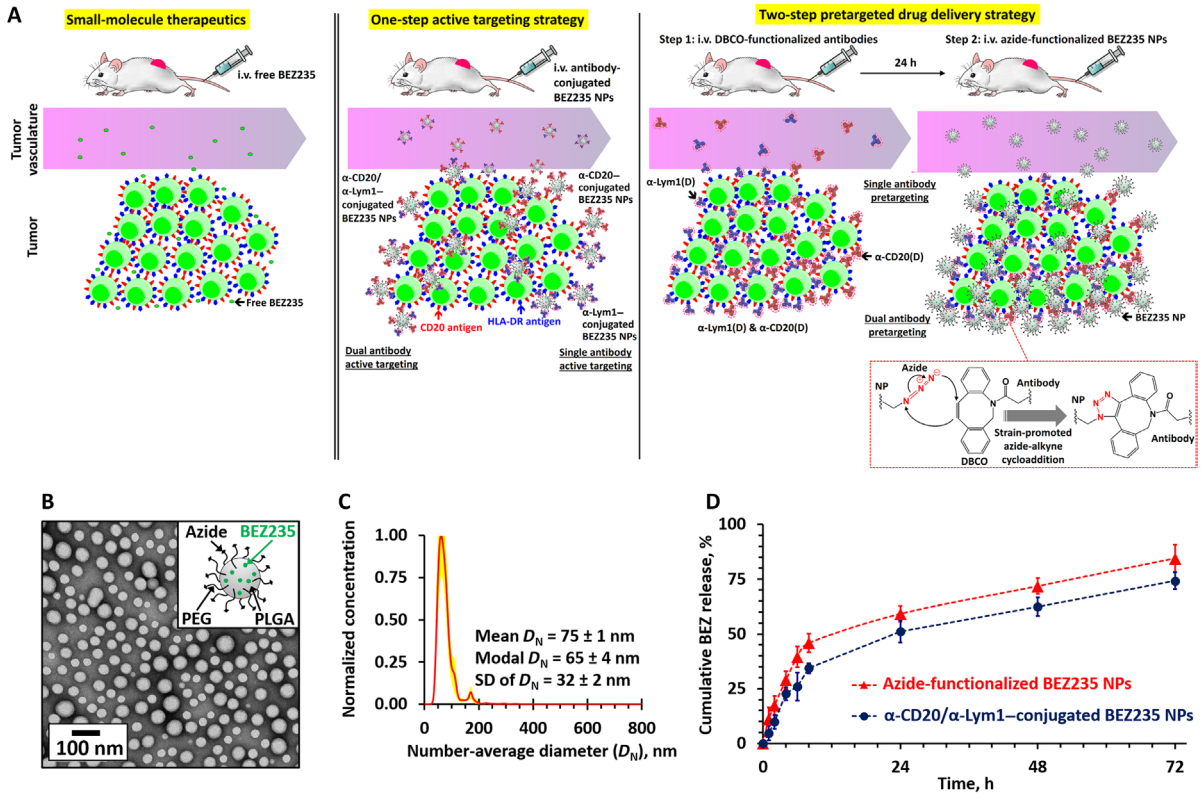

Fig. 1. Mechanism of action and characterization of active targeted and pretargeted BEZ235 NPs. (**A**) Active targeting and pretargeting mechanisms of different BEZ235 nanoformulations. i.v., intravenous. (**B**) TEM image of azide-functionalized BEZ235 NPs. The inserted cartoon illustrates the structure of BEZ235 NPs. Hydrophobic BEZ235 was encapsulated inside the hydrophobic PLGA core of the diblock copolymer NPs. (**C**) Number-average distribution curve of BEZ235 NPs as determined by NP tracking analysis (NTA) method. (**D**) In vitro drug release study of nonfunctionalized and Ab-conjugated BEZ235 NPs at physiological conditions [0.1 M PBS (pH 7.4), 37°C].

Ab pretargeted treatment strategy can effectively inhibit the tumor growth and prolong the survival of tumor-bearing mice through inhibition of the PI3K/mTOR pathway. Biodistribution studies confirm that more NPs are accumulated at the target tumor site via the dual Ab pretargeted strategy than the single Ab pretargeted strategy. We further demonstrate that the NP-based pretargeted strategy notably reduces the toxic effects on normal tissues associated with the systemic administration of BEZ235.

RESULTS

Development of two-component bioorthogonal pretargeted system for the delivery of BEZ235 nanoformulation to CD20- and HLA-DR–expressing lymphoma cells

A two-component pretargeted drug delivery system has been developed for the therapeutic delivery of a BEZ235 nanoformulation to CD20- and HLA-DR–overexpressing lymphoma cells. The tumor-targeting Abs [α-CD20(D) and α-Lym1(D)] were functionalized with an average of eight DBCO ligands (fig. S2). The therapeutic effector, 70-nm-diameter azide-functionalized BEZ235 NPs (Fig. 1, B and C), was encapsulated with approximately 1.3% (w/w) of BEZ235 [NPs (13 μg/mg)]. The encapsulated BEZ235 demonstrated controlled release at physiological conditions (Fig. 1D). Single and dual Ab–conjugated BEZ235 NPs that also undergo controlled release under physiological conditions were prepared (Fig. 1C). Rhodamine-labeled NPs (Rhod NPs) and Cy5-labeled NPs (Cy5 NPs) were prepared for in vitro binding and in vivo biodistribution studies, respectively. Their physicochemical properties are summarized in figs. S3 and S4.

In vitro binding assay

A fluorescence-activated cell sorting (FACS) cell binding assay was performed in all four lymphoma cell lines with different CD20 and HLA-DR antigen densities (fig. S1). This experiment verified that the pretargeted strategy is more effective than active targeting when NPs target tumor cells under excess conditions (Fig. 2A). In the high CD20- and HLA-DR–expressing Raji and Daudi cells, the single Ab pretargeted method notably increased the amount of Rhod NPs retained on the surface of cancer cells compared with single Ab–conjugated NPs. Dual Ab pretargeted Rhod NPs using half amount of each Ab was as efficient as single Ab pretargeted Rhod NPs to label the Raji and Daudi cells. Conversely, the same concentration α-CD20/α-Lym1–conjugated Rhod NPs and α-CD20–conjugated Rhod NPs plus α-Lym1–conjugated Rhod NPs did not notably enhance the mean fluorescence intensities versus single Ab–labeled NPs. A similar enhancement effect was observed in the Namalwa and Ramos cells, but enhancement effects were diminished because of lower CD20 and HLA-DR densities in both cell lines. In addition, nonspecific binding was found in the negative control Jurkat cells after being incubated with the direct Ab-conjugated Rhod NPs, while the pretargeted formulations show no evidence of nonspecific

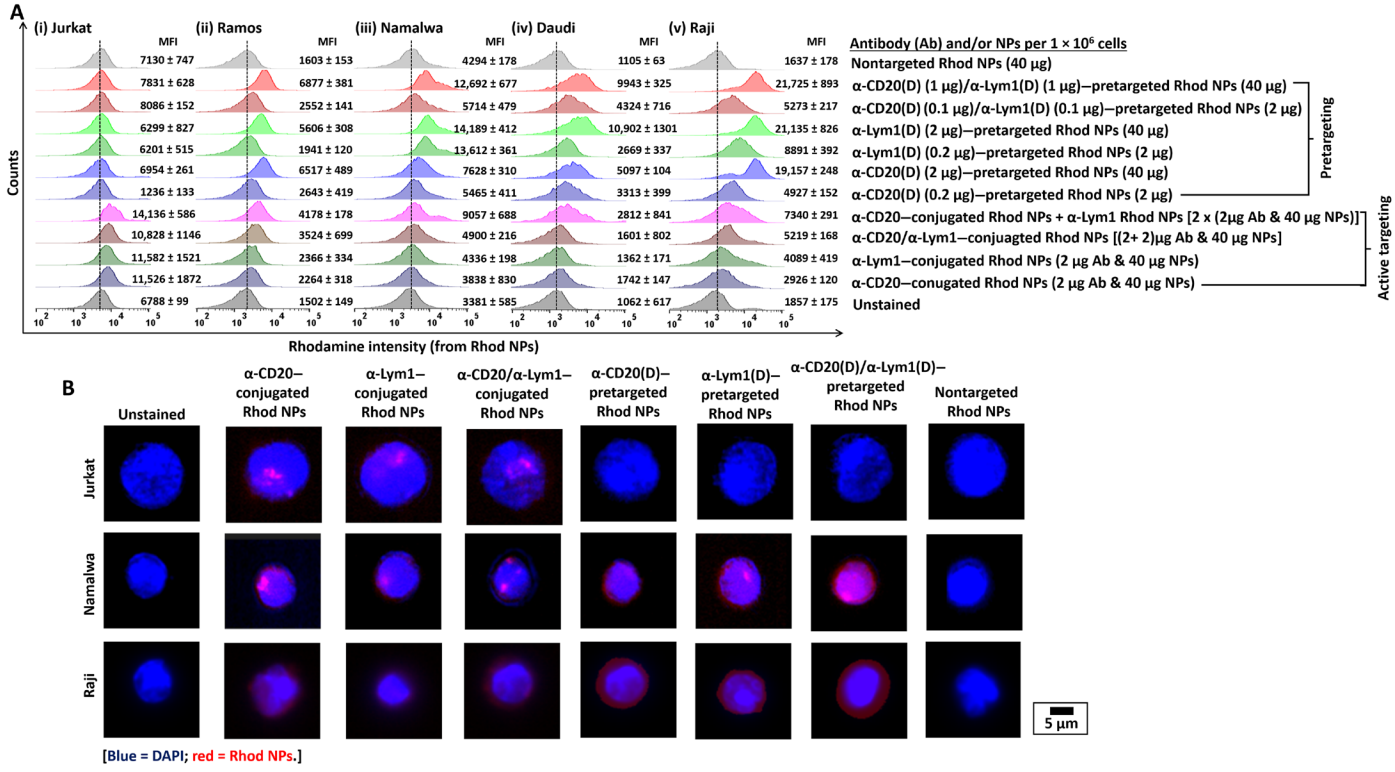

Fig. 2. Dual Ab pretargeted strategy increases the number of effector Rhod NPs retained on lymphoma cells. (**A**) Representative FACS histograms of Jurkat ($CD20^-$ and $HLA\text{-}DR^-$), Ramos, Namalwa, Daudi, and Raji cells after staining with Rhod NPs via active targeting and pretargeting methods. (**B**) Representative high-magnification fluorescence images of Raji cells after staining with different Rhod NPs via active targeting or pretargeting methods.

binding to Jurkat cells. The binding of the Rhod NPs through the pretargeted strategy was further confirmed by fluorescence microscopy, with a ring-like pattern of staining observed (Fig. 2B).

In vitro cytotoxicity assay

To verify that the pretargeted strategy can enhance the antitumor activities of BEZ235, we performed comprehensive in vitro cytotoxicity studies to assess the proliferation of lymphoma cells after treatment with free BEZ235 and the six different BEZ235 nanoformulations (Fig. 3A and fig. S5). All four lymphoma cells were sensitive to free BEZ235 treatment, with IC_{50} values between 40 and 160 nM. α-CD20/α-Lym1 pretreatment did not significantly change the IC_{50} values of free BEZ235 in all four lymphoma cells. Nontargeted BEZ235 NPs and drug-free Ab-conjugated NPs showed insignificant in vitro toxicities. All three single/dual Ab–conjugated BEZ235 NPs exhibited moderate antitumor activities, but most of their IC_{50} values (for the encapsulated BEZ235) increased to above 10 μM. The pretargeted treatment method, especially treatment with the α-CD20(D)/α-Lym1(D) dual pretargeted BEZ235 NPs, significantly enhanced in vitro cytotoxicity of the BEZ235 nanoformulations (IC_{50} = 40 to 90 nM). Control studies confirmed that the pretargeted approach with the same doses of drug-free NPs had no significant toxicity. Further Western blot analyses of Namalwa and Raji cells (Fig. 3B and figs. S6 and S7) confirmed that both pretargeted treatments were as efficient as free BEZ235 in inhibiting the phosphorylation of AKT (S473) and S6 ($Ser^{240/244}$), the downstream targets of the PI3K and mTOR signaling cascades, in a time-dependent manner in vitro.

In vivo NP uptake and biodistribution studies

Time-dependent tumor uptake studies were evaluated using Raji xenograft tumor model to confirm that the NP-based pretargeted strategy can enhance the uptake of the Cy5 NPs (Fig. 4A and fig. S8). The mean epifluorescence intensities (MEIs) of the xenograft tumors rapidly increased and reached a maximum at 30 min after injection of the nontargeted Cy5 NPs (Fig. 4A). The MEIs dropped exponentially over time and returned to background levels 24 hours after administration (Fig. 4Aand fig. S8). Conversely, the MEIs of the xenograft tumors remained relatively constant in the first 8 hours after the administration of the directly Ab-conjugated Cy5 NPs (Fig. 4Aand fig. S8), although the MEI gradually declined over time thereafter. In contrast to the directly Ab-conjugated NPs, the MEIs of the pretargeted tumors reached a maximum 3 hours after injection and were maintained for another 5 hours (Fig. 4A and fig. S8). The maximum MEIs of single Ab pretargeted tumors were twofold higher than that of directly Ab-conjugated Cy5 NPs (after subtracting the background MEI; Fig. 4A). Furthermore, the maximum MEIs of dual Ab (i.e., α-CD20 and α-Lym1) pretargeted tumors were approximately 50% higher than that of single Ab (i.e., α-CD20 or α-Lym1) pretargeted tumors (Fig. 4A).

Further ex vivo biodistribution study confirmed that the NP-based pretargeted strategy significantly increased the amount of Cy5 NPs retained in the Raji tumor (Fig. 4B and fig. S9). Approximately 23% ID/g of the dual Ab pretargeted Cy5 NPs were retained in the tumor (Fig. 4B) at 48 hours after the intravenous administration, which was about a 40 to 60% increase in tumor uptake compared to the

A

	Half-maximal inhibitory concentration (IC_{50}), μM			
	Ramos	Namalwa	Daudi	Raji
Free BEZ235	0.04 ± 0.01	0.14 ± 0.02 μM	0.04 ± 0.01 μM	0.16 ± 0.05 μM
α-CD20/α-Lym1 followed by free BEZ235	0.04 ± 0.01	0.13 ± 0.01 μM	0.02 ± 0.01 μM	0.08 ± 0.01 μM
Nontargeted BEZ235 NPs	> 10	> 10 μM	> 10 μM	> 10 μM
α-CD20	> 0.05	> 0.05 μM	> 0.05 μM	> 0.05 μM
α-Lym1	> 0.05	> 0.05 μM	> 0.05 μM	> 0.05 μM
1:1 α-CD20/α-Lym1	> 0.05	> 0.05 μM	> 0.05 μM	> 0.05 μM
α-CD20–conjugated BEZ235 NPs	> 10	> 10	> 10	> 10
α-Lym1–conjugated BEZ235 NPs	> 10	> 10	> 10	> 10
α-CD20/α-Lym1–conjugated BEZ235 NPs	> 10	> 10	> 10	9.36 ± 0.59
α-CD20(D)–pretargeted BEZ235 NPs	0.09 ± 0.01	0.08 ± 0.01	0.08 ± 0.01	0.06 ± 0.01
α-Lym1(D)–pretargeted BEZ235 NPs	0.10 ± 0.01	0.16 ± 0.01	> 10	0.11 ± 0.01
α-CD20(D)/α-Lym1(D)–pretargeted BEZ235 NPs	0.09 ± 0.01	0.05 ± 0.01	0.03 ± 0.01	0.04 ± 0.01

B

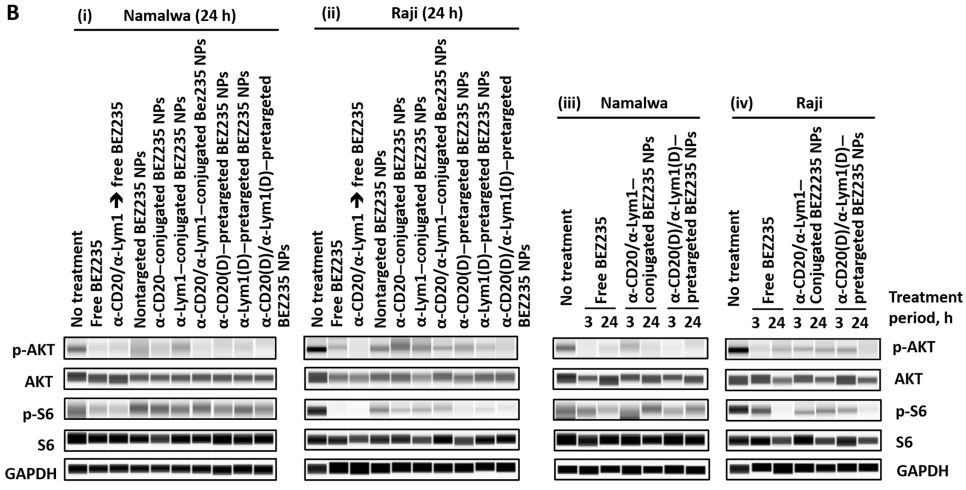

Fig. 3. In vitro toxicity of free BEZ235 and different BEZ235 nanoformulations. (**A**) The table summarizes IC_{50}s of free BEZ235 and different BEZ235 nanoformulations in Ramos, Namalwa, Daudi, and Raji cell lines. BEZ235 nanoformulations, except nontargeted BEZ235 NPs, were delivered via active targeting and pretargeting methods [N.B. BEZ235 (375 μg/ml) NPs contained 10 μM encapsulated BEZ235]. Drug-free NPs showed insignificant toxicities in all four cell lines (fig. S5, iii and v). (**B**) Auto-Western blot analysis on p-AKT, AKT, p-S6, S6, and GAPDH protein expressions in Namalwa and Raji cells after being treated with 500 nM free BEZ235 or different BEZ235 nanoformulations for 3 or 24 hours.

single Ab pretargeted NPs. All three directly Ab-conjugated Cy5 NPs were also retained in the tumor (6 to 11% ID/g) at 48 hours after injection, but they were more than twofold less effective than the pretargeted NPs (Fig. 4B), with most of the administered NPs accumulated in the liver (18 to 20% ID/g, which was roughly 40% of all administered NPs; Fig. 4B). Small amounts of Cy5 NPs were also found in the kidney and spleen across different treatment groups. Histological analyses confirmed that a ring-like pattern of labeling can be observed in the preserved Raji tumor sections following the administration of pretargeted Cy5 NPs (Fig. 4C) that attribute to the specific binding to the CD20 and HLA-DR antigens.

In vivo antitumor efficacy study

In vivo antitumor efficacy evaluation was carried out by using Namalwa and Raji xenograft models to determine the antitumor activities of various BEZ235 formulations. In the Namalwa tumor model (Fig. 5, A and B, and figs. 10 and 11), both free BEZ235 and nontargeted BEZ235 NPs exhibited moderate antitumor activities with tumor growth inhibition (TGI) of 29% ($P = 0.0214$ versus nontreatment group) and 46% ($P = 0.0156$ versus nontreatment group), respectively. Treatment with free α-CD20 or free α-Lym1 Abs did not show significant antitumor activities ($P = 0.1563$ and 0.5010 versus nontreatment group, respectively; fig. S11). Pretreatment with α-CD20 and/or α-Lym1 did not significantly affect the antitumor activities of free BEZ235 and BEZ235 NPs (fig. S11). Treatment with directly Ab-conjugated BEZ235 NPs slightly improved the antitumor activity versus the nontargeted BEZ235 NPs ($P = 0.0313$ and 0.0781 versus nontreatment group, respectively, for α-CD20 or α-Lym1; fig. S11). Treatment with α-CD20(D) or α-Lym1(D) single pretargeted BEZ235 NPs effectively inhibited tumor growth and resulted in TGIs of 65 and 74% ($P = 0.0481$ and 0.0313 versus treatment with BEZ235 NPs), respectively. The antitumor activity increased further in the α-CD20(D)/α-Lym1(D) dual pretargeted BEZ235 NPs and resulted in a TGI of 76% ($P = 0.0313$ versus treatment with nontargeted BEZ235 NPs). In addition, the NP-based pretargeted strategy, especially the dual Ab pretargeting strategy, significantly prolonged survival [median survival (MS) = 43 to 48 days; Fig. 5C] compared with free BEZ235 (MS = 31 days; fig. S12) and nontargeted BEZ235 NPs (MS = 31 days; fig. S12).

In the more aggressive Raji tumor model, mice did not respond to most Ab, single/dual Ab–conjugated BEZ235 NPs, and small-molecule drug treatments (Fig. 6, A to B, and figs. S13 to S15). Treatment with α-CD20(D) or α-Lym1(D) single pretargeted BEZ235 NPs significantly inhibited tumor growth and resulted in TGIs of 55 and 39% ($P = 0.0156$ and 0.0156 versus nontreatment group), respectively. Treatment with the α-CD20(D)/α-Lym1(D) dual pretargeted BEZ235 NPs further inhibited tumor growth and resulted in a TGI of 80% ($P = 0.0025$ versus nontreatment group; Fig. 6B). In addition, dual

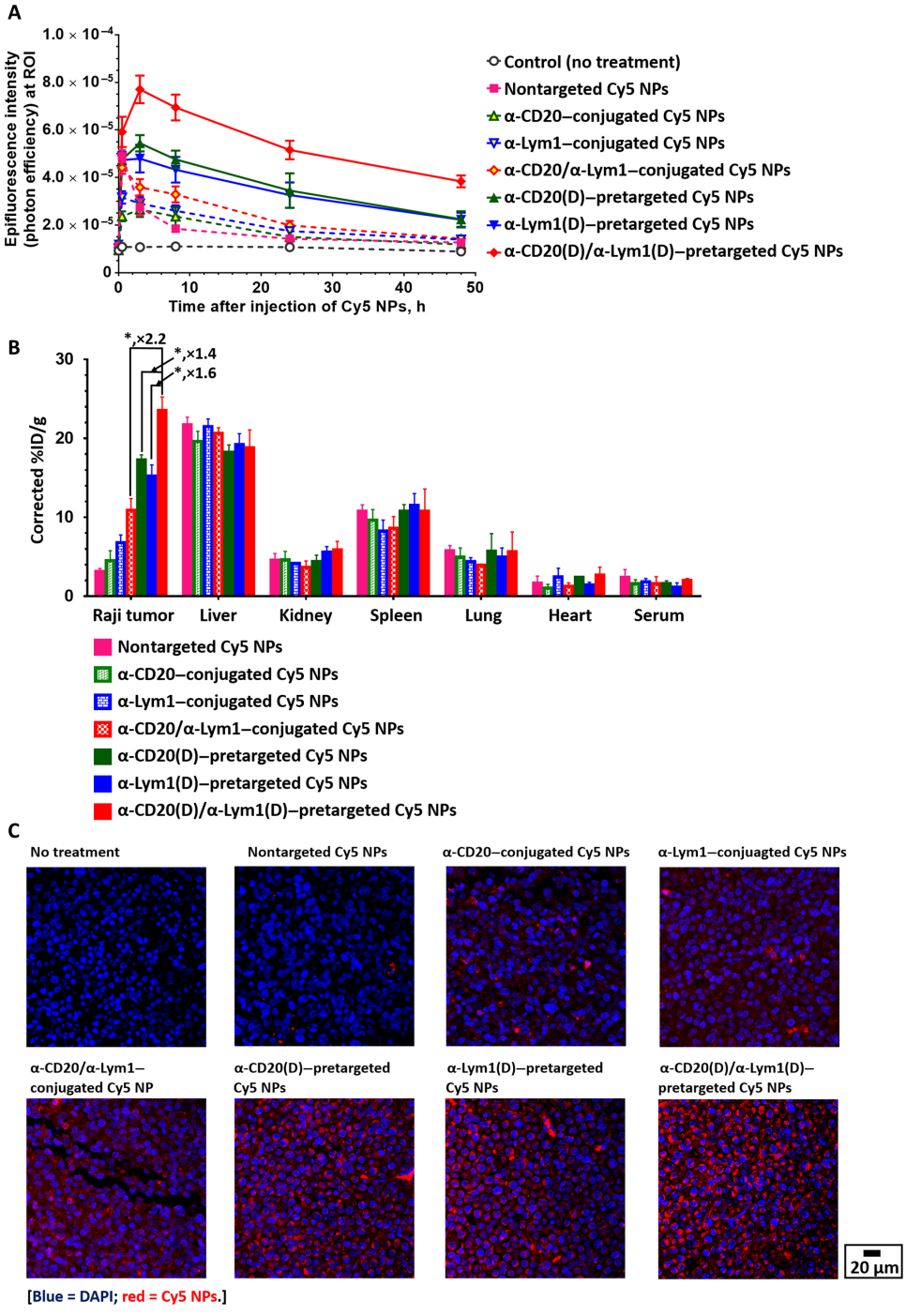

Fig. 4. In vivo uptake and biodistribution of active targeted and pretargeted Cy5 NPs in Raji xenograft tumor model. (**A**) Time-dependent epifluorescence intensities of Raji xenograft tumor recorded after intravenous administration of different active targeted and pretargeted Cy5 NPs ($n = 5$). ROI, region of interest. (**B**) Biodistribution of different active targeted and pretargeted Cy5 NPs quantified 48 hours after intravenous administration (N.B., $n = 5$, $^*P < 0.05$). (**C**) Representative confocal laser scanning microscopy images of Raji xenograft tumor preserved 48 hours after intravenous administration of different Cy5 NPs.

pretargeted treatment with BEZ235 NPs significantly increased the MS to 52 days (versus 31 days recorded for the nontreatment group and nontargeted BEZ235 NPs treatment group; Fig. 6C). Furthermore, negative control studies confirmed that single/dual Ab pretargeted drug-free NPs had insignificant anticancer activities compared with the nontreatment group and the single/dual Ab treatment groups (figs. S13B, S14B, and S15B). Further histopathological analyses confirmed that the Raji tumor treated with the dual pretargeted BEZ235 NPs had significantly less phosphorylated ribosomal S6 protein expression (Fig. 6D and fig. S16). This finding confirms that the antitumor activity was due to the inhibition of the PI3K/mTOR pathway from BEZ235.

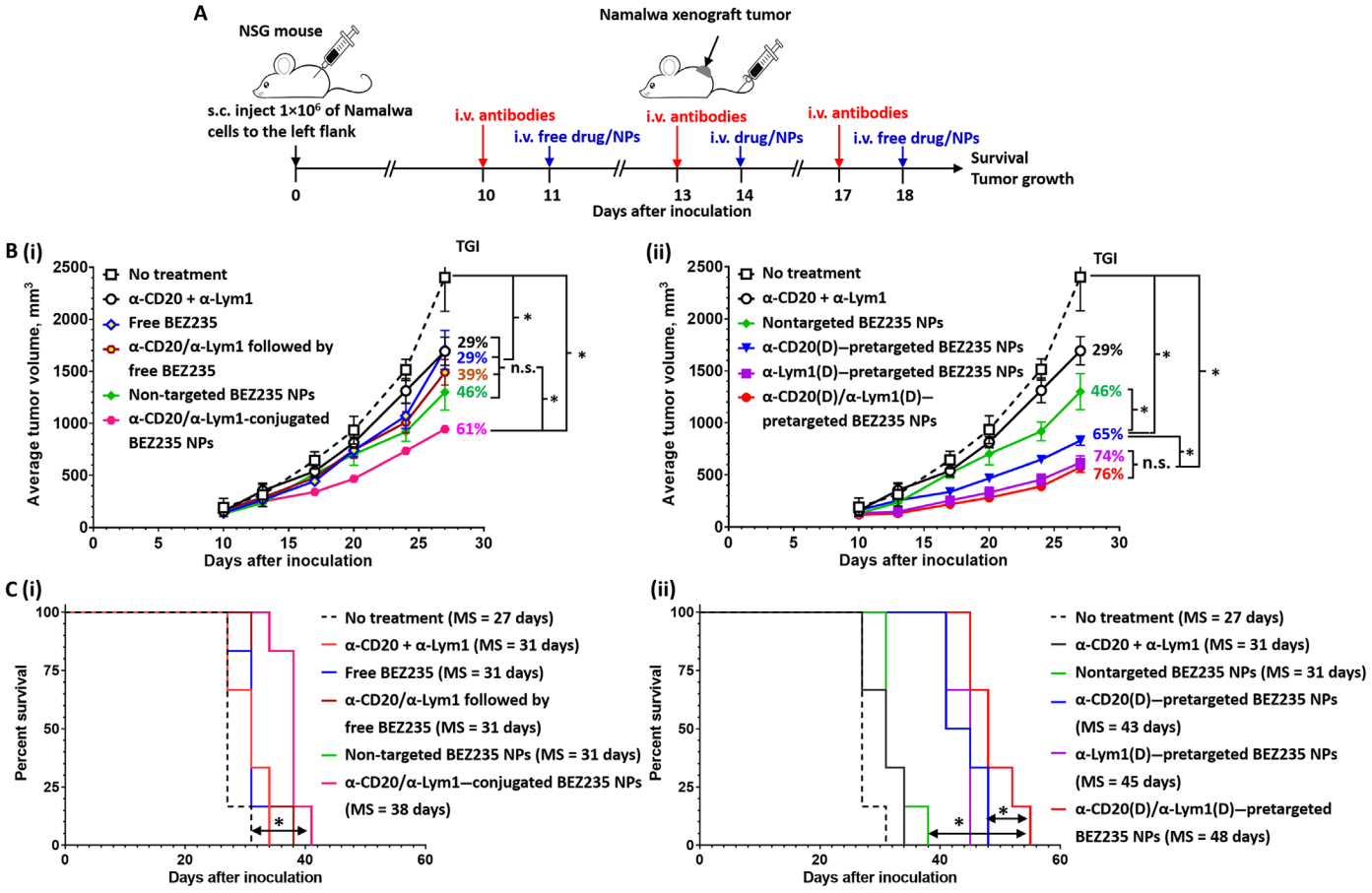

Fig. 5. In vivo antitumor activities of free BEZ235 and different BEZ235 nanoformulations in Namalwa xenograft tumor model. (**A**) Treatment schedule. Abs (total, 100 μg per treatment) were intravenously (tail vein) administered at days 10, 13, and 17 after inoculation, and free BEZ235 and BEZ235 nanoformulations (51 μg of free BEZ235 or 5 mg of BEZ235 NPs per treatment) were intravenously administered on days 11, 14, and 18 after inoculation. s.c., subcutaneous. (**B**) Average tumor growth curves recorded for nontreatment group mice and mice that received different nontargeted or targeted treatments. TGI was calculated 10 days after final drug treatment. (**C**) Survival curves and MS were recorded for nontreatment group mice as well as mice that received different nontargeted or targeted treatments ($n = 6$ to 7 per group; n.s. denotes $P > 0.05$ and $^*P < 0.05$).

In vivo toxicity

The in vivo toxicities of free BEZ235 and all three BEZ235 nanoformulations delivered through direct targeting or pretargeting strategies were assessed in healthy CD-1 mice. Mice that were administered a therapeutic dose of free BEZ235 and free α-CD20/free α-Lym1 Abs followed by free BEZ235 (24 hours apart) showed elevated serum aspartate aminotransferase (AST), blood urea nitrogen (BUN), and creatinine levels 48 hours after administration (Fig. 7A). This indicates that free BEZ235 induced notable liver and kidney damages. Conversely, administration of the three different BEZ235 nanoformulations showed no notable hepatotoxicity or nephrotoxicity (Fig. 7A). Further serum analyses (fig. S17) suggested that the administration of free BEZ235 formulations significantly reduced the total number of white blood cells and lymphocyte counts. Conversely, mice that received the BEZ235 nanoformulations did not show significant hematological toxicity except for a slight reduction in platelet count (fig. S17). Further histological study from necropsy confirmed that the administration of free BEZ235 induced notable liver and lung inflammation as well as renal cortical necrosis (Fig. 7B). None of the BEZ235 nanoformulations induced substantial histological abnormalities in any key organs.

DISCUSSION

Targeted therapy using small-molecule inhibitors have led to a paradigm shift in the treatment of cancer. Overactivation of the PI3K/mTOR signaling pathway has been identified as one of the key regulators of cell growth and survival in a number of hematological malignancies, including NHL, and it has been actively investigated as a target for small-molecule inhibitors. There are currently three PI3K small-molecule inhibitors (i.e., idelalisib, copanlisib, and duvelisib) approved by the U.S. Food and Drug Administration for treatment of NHL. A landmark clinical trial in relapsed or refractory chronic lymphocytic leukemia showed that idelalisib, in combination with rituximab, produced a very high overall response rate of 81% with 1-year overall survival of 92% (*32*).

Despite the promising efficacy data associated with PI3K inhibitors, their clinical use is hampered by poor cancer-targeting specificity as well as on-target/off-tumor side effects, including hepatitis, colitis, and pneumonitis (*19*, *20*, *22*). Specifically, more than 60% of patients suffer grade 3 or 4 side effects in combination targeted therapy with these PI3K inhibitors (*25*). BEZ235 is another small-molecule inhibitor targeting PI3K pathway with promising antitumor activity in various cancer models in vivo, but its oral formulation has been

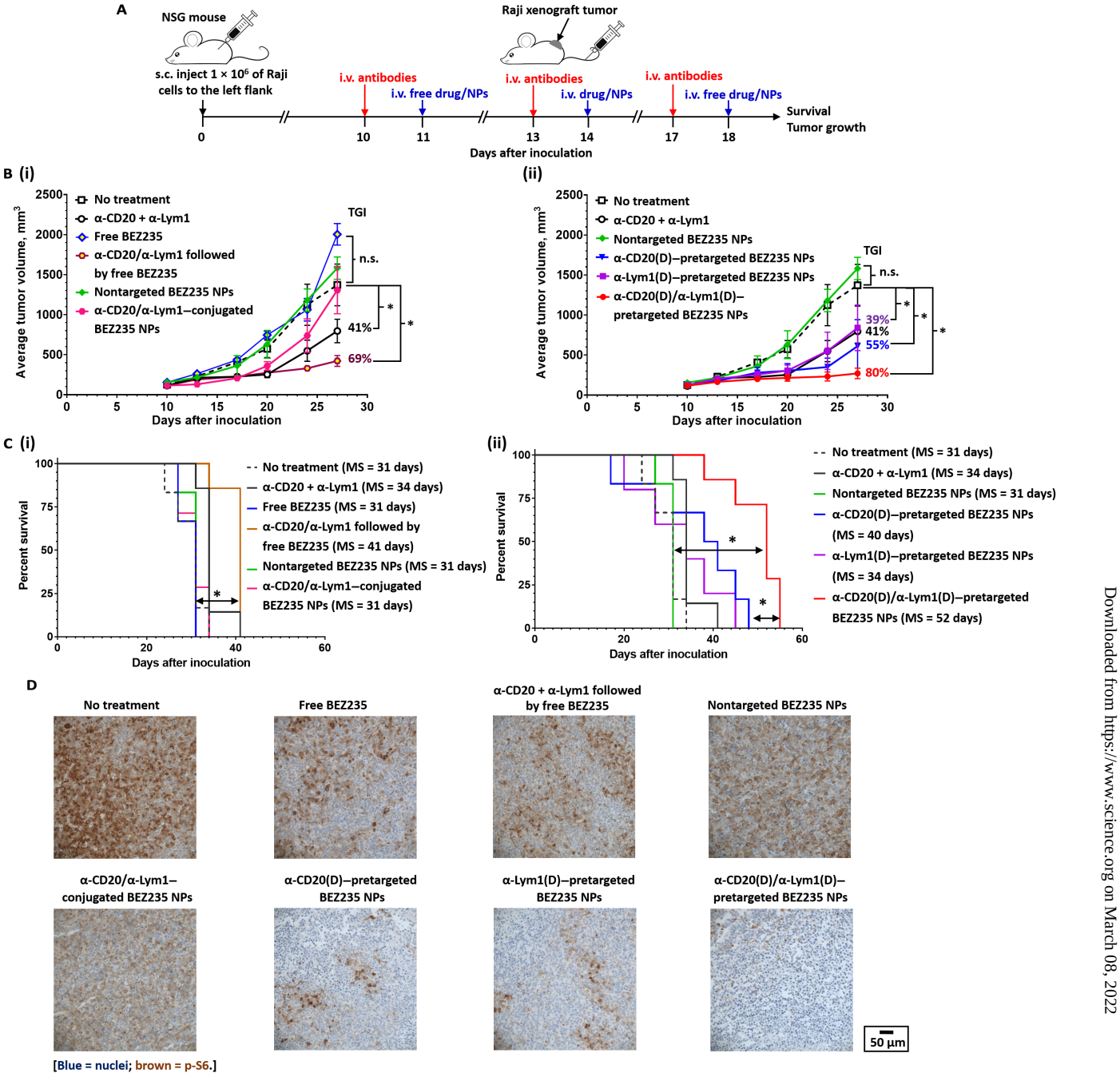

Fig. 6. In vivo antitumor activities of free BEZ235 and different BEZ235 nanoformulations in Raji xenograft tumor model. (**A**) Treatment schedule. Raji xenograft tumors were inoculated by subcutaneous injection of 1×10^6 of Raji cells to the left flank. Abs (total, 100 μg per treatment) were intravenously administered at days 10, 13, and 17 after inoculation, and free BEZ235 and different BEZ235 nanoformulations (51 μg of free BEZ235 or 5 mg of BEZ235 NPs per treatment) were intravenously administered at days 11, 14, and 18 after inoculation. For the pathological study, Abs (total, 100 μg per treatment) were administered at day 10, and free BEZ235 and BEZ235 nanoformulations (51 μg of free BEZ235 or 5 mg of BEZ235 NPs per treatment) were administered at day 11. Xenograft tumors were preserved at day 14 (3 days after drug treatment). (**B**) Average tumor growth curves were recorded for nontreatment group mice as well as mice that received different nontargeted, active targeted, and pretargeted treatments. (**C**) Survival curves and MS recorded for nontreatment group mice as well as mice that received different nontargeted, active targeted, and pretargeted treatments. (**D**) Representative immunohistochemistry images of anti–p-S6–stained Raji tumor sections after receiving different types of BEZ235 treatments ($n = 6$ to 7 per group; n.s. denotes $P > 0.05$ and $^*P < 0.05$).

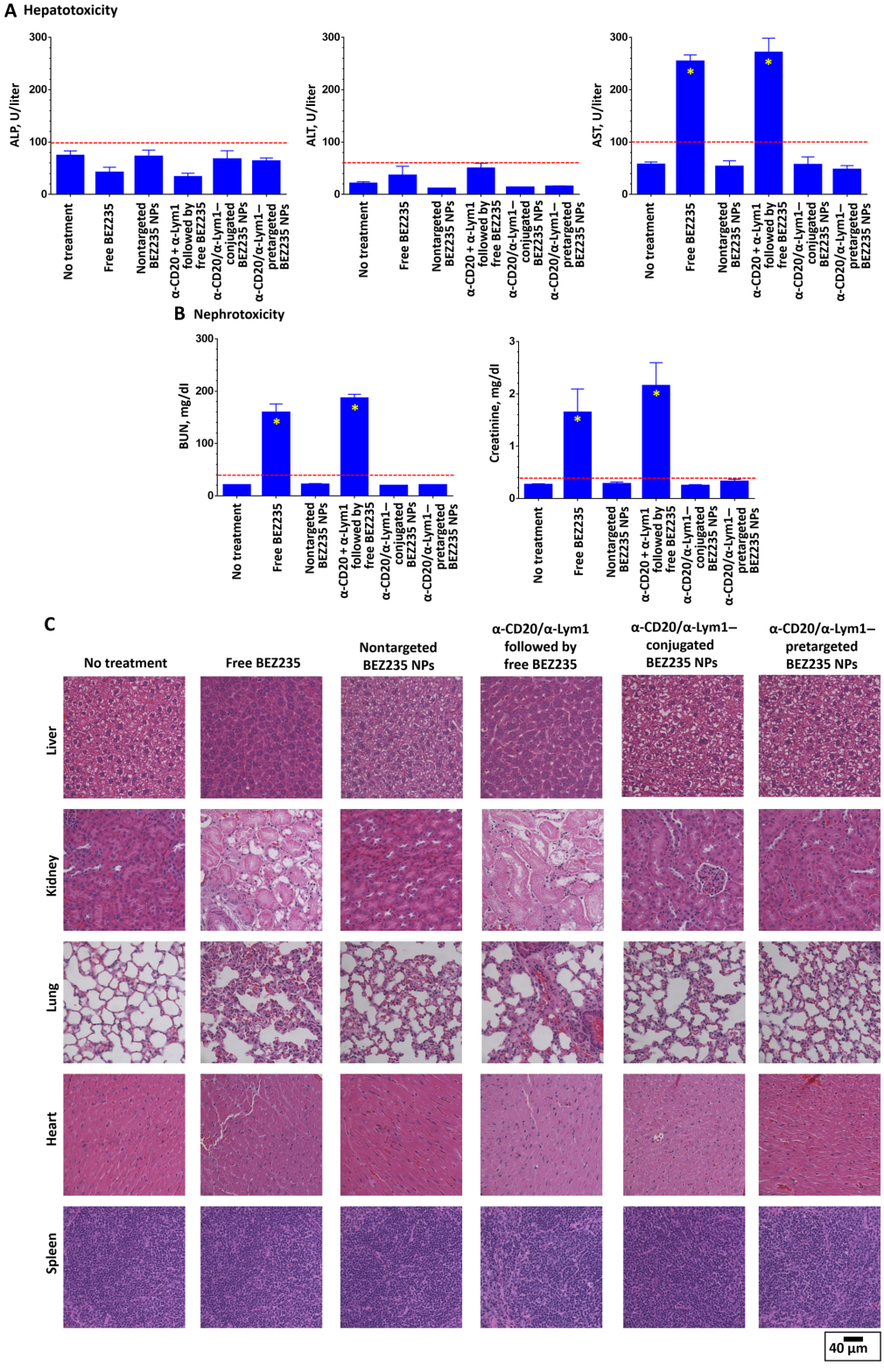

Fig. 7. In vivo toxicities of free BEZ235 and different BEZ235 nanoformulations evaluated in healthy CD1 mice. Mice were intravenously administrated with a total of 100 μg of Abs followed by 50 μg of free or encapsulated BEZ235. Full blood was collected 48 hours after intravenous administration of BEZ235 for hepatotoxicity, nephrotoxicity, and hematological toxicity studies. Key organs (liver, kidney, lung, heart, and spleen) were preserved for pathological studies. (**A**) Serum alkaline phosphate (ALP), alanine aminotransferase (ALT), and aspartate aminotransferase (AST) levels recorded for mice in nontreatment and treatment groups (N.B., $n = 5$, * denotes abnormal). (**B**) Blood urea nitrogen (BUN) and creatinine levels were recorded for mice in nontreatment and treatment groups (N.B., $n = 5$, * denotes abnormal). (**C**) Hematoxylin and eosin–stained images of liver, kidney, lung, heart, and spleen sections were preserved from mice in nontreatment and treatment groups.

limited by poor bioavailability and serious adverse events in phase 1/2 trials (*28*, *29*). In the current preclinical study, we investigated the use of an NP-based pretargeted drug delivery system to improve the therapeutic window of BEZ235 for treatment of NHL.

A multistep pretargeted delivery strategy was initially explored for radioimmunotherapy of relapsed NHL (*33*). The key goals of pretargeted radioimmunotherapy are to increase the tumor uptake of the radionuclide and reduce nonspecific uptake in the vital organs (*33*–*35*). However, the multistep pretargeted treatment strategy has not been widely used in clinical settings because of the immunogenic nature of many pretargeting protein tags (e.g., streptavidin) and technical difficulties of delivering radionuclides (*33*–*35*). Our recent study demonstrates that these challenges can be overcome by using NP-based bioorthogonal strain-promoted alkyne-azide cycloaddition between fully synthetic ligands (e.g., DBCO and azide) (*15*). In the current study, in vitro binding studies in four established lymphoma cell lines confirmed that the DBCO- and azide-based pretargeting strategy can increase the amount of effector NPs retained in the target tumor cells compared with directly Ab-conjugated NPs. We also showed that dual Ab pretargeting using two different Abs, which recognize different tumor-associated antigens, can increase the amount of effector NPs retained in the target cells due to the increased number of tumor-associated antigen density available for NP binding (*36*). The enhancement effect was further confirmed through ex vivo biodistribution study using the Raji tumor model, in which the dual Ab pretargeting method increased the uptake of effector NPs by approximately 35% compared with the single Ab pretargeting method, and the NP uptake was doubled compared to directly Ab-conjugated NPs targeting both antigens.

The improved in vitro and in vivo uptake of the effector NPs successfully translated to enhanced antitumor activities of the pretargeted BEZ235 nanoformulations. The dual Ab pretargeted BEZ235 nanoformulation inhibited tumor growth by approximately 80% in the Namalwa and Raji tumor models, whereas free BEZ235 showed only modest antitumor activity when combined with α-CD20 and α-Lym1 Abs in the Namalwa tumor model and minimal antitumor activity in the more aggressive Raji tumor model. The mechanistic study here indicated that all BEZ235 nanoformulations had slower but more durable inhibition of the PI3K/mTOR pathway versus free BEZ235. In addition to the improved antitumor activity, the NP-enabled pretargeted delivery strategy also notably reduced the on-target/off-tumor toxicities due to rapid elimination of BEZ235 NPs by the Kupffer cells through the recently identified hepatobiliary elimination pathway (*37*).

In summary, we report a novel dual Ab pretargeted drug delivery system based on DBCO-functionalized α-CD20 and α-Lym1 Abs and azide-functionalized BEZ235-encapsulated NPs targeting NHL. Using four established lymphoma cell lines, our data demonstrate that the NP-enabled pretargeted strategy is more effective than free BEZ235 as well as directly Ab-conjugated BEZ235 NPs for inhibiting the PI3K/mTOR pathway in vitro and in vivo. Our findings also show that the dual Ab pretargeting method is more effective than the single Ab pretargeting method for delivering the effector vehicles to target tumor cells by improving NP uptake via increased antigen density for target binding. Last, the pretargeted BEZ235 nanoformulations effectively reduced the toxicities associated with systemic administration of BEZ235. To the best of our knowledge, this is the first study to investigate the use of a pretargeted method to improve the efficacy and safety of small-molecule inhibitors. The novel design of this pretargeted system has broad applicability to other malignancies by allowing easy exchange of the tumor-targeting moiety and therapeutic effectors to target different tumor surface markers as well as various signaling pathways.

MATERIALS AND METHODS

Materials

BEZ235 was purchased from LC Laboratories. Mouse anti-human CD20 Ab [clone: 2H7; isotype: mouse immunoglobulin G2b (IgG2b); InVivoMAb grade] and anti-mouse NK1.1 Ab (clone: PK135; isotype: mouse IgG2a; InVivoMAb grade) were purchased from BioXCell (West Lebanon, NH). Mouse anti-human Lym1 Ab (isotype: mouse IgG2a) was extracted from Lym1 cells [American Type Culture Collection (ATCC) HB-8612] by the Protein Expression and Purification Core at the University of North Carolina (UNC) School of Medicine according to a published protocol (*38*). Poly(lactide-*co*-glycolide)-*b*-poly(ethylene glycol)-azide copolymer (AI091), methoxy poly(ethylene glycol)-*b*-poly(D,L-lactic-*co*-glycolic) acid copolymer (AK101), poly(lactide-*co*-glycolide)-rhodamine B (AV011), and poly(D,L) lactic acid-cyanine 5 endcap (AV032) were purchased from Akina Inc. (West Lafayette, IN).

Cell lines

Jurkat, Ramos, Namalwa, Daudi, and Raji cell lines were obtained from the Tissue Culture Facility at the UNC Lineberger Comprehensive Cancer Center (purchased from ATCC). Cells were cultured in RPMI 1640 medium (Gibco) supplemented with 10% fetal bovine serum (FBS; VWR Life Science Seradigm) and antibiotic-antimycotic (Gibco) in a humidified atmosphere incubator (at 37°C and 5% CO_2).

Functionalization of α-CD20 and α-Lym1 Abs

α-CD20 and α-Lym1 were functionalized via amine-NHS (*N*-hydroxysuccinimide) ester coupling reactions. For the preparation of α-CD20 (DL488) and α-Lym1 (Texas Red), α-CD20 and α-Lym1 (5 mg/ml) were functionalized with DyLight 488 NHS ester (Thermo Fisher Scientific) and Texas Red NHS ester (Thermo Fisher Scientific), respectively, at a 1:4 Ab-to-dye molar ratio. Both Abs were functionalized at pH 8.0 at 20°C (in the dark) for 2 hours. Dye-functionalized Abs were purified by disposable PD-10 Desalting Columns (GE Healthcare) according to the manufacturer's protocol. The concentration and degree of functionalization of both Abs were determined by ultraviolet (UV)–visible spectroscopy using a NanoDrop 1000 spectrophotometer. Briefly, the concentrations and degrees of the DyLight 488 and Texas Red incorporation to the α-CD20 and α-Lym1 Abs were determined spectroscopically using an absorption coefficients of 70,000 M^{-1} liter cm^{-1} and 80,000 M^{-1} liter cm^{-1}, an absorption coefficient of mouse immunoglobulin at 280 nm ($\varepsilon_{280\ nm}$) = 1.33 mg^{-1} ml cm^{-1}, and DyLight 488 and Texas Red correction factors at 280 nm of 0.147 and 0.18 according to the manufacturer's instructions.

DBCO-functionalized Abs were prepared via same amine-NHS ester coupling reaction with DBCO-PEG13-NHS ester (Click Chemistry Tools, Scottsdale, AZ) at pH 8.0. The target degree of functionalization for both Abs was 20. DBCO-functionalized Abs were purified by disposable PD-10 Desalting Columns (GE Healthcare) according to the manufacturer's protocol. The concentration and degree of functionalization of both Abs were determined by UV-visible spectroscopy using a NanoDrop ND-1000 UV-visible spectrophotometer (Thermo

Fisher Scientific). Briefly, the concentrations and degrees of the DBCO incorporation of different purified DBCO-conjugated Abs were determined spectroscopically using an absorption coefficient of DBCO at 310 nm ($\varepsilon_{DBCO,310\ nm}$) = 12,000 M^{-1} liter cm^{-1}, an absorption coefficient of mouse immunoglobulin at 280 nm ($\varepsilon_{280\ nm}$) = 1.33 mg^{-1} ml cm^{-1}, and a DBCO correction factor at 280 nm ($CF_{DBCO,280\ nm}$) = 1.089 according to the manufacturer's instructions.

Preparation and characterization of BEZ235 NPs

BEZ235 NPs were prepared via a nanoprecipitation method. The target drug loading was 5% (w/w). For the preparation of 300 mg of BEZ235 NPs, 15 mg of free BEZ235 was first dissolved in 3 ml of warm dimethyl sulfoxide (DMSO) before being added to a polymer blend that contained 100 mg of poly(lactide-*co*-glycolide)-*b*-poly(ethylene glycol)-azide copolymer (AI091, Akina Inc.) and 300 mg of methoxy poly(ethylene glycol)-*b*-poly(lactide-*co*-glycolide) (AK101, Akina Inc.) dissolved in 100 ml of acetonitrile. The polymer blends were then added slowly (1 mg/min) into 400 ml of molecular biology–grade deionized water (Corning) with constant stirring (1000 rpm). The mixture was then stirred under reduced pressure for 15 hours in the dark. The BEZ235 NPs were purified with an Amicron Ultra ultrafiltration membrane filter [molecular weight cutoff (MWCO), 50,000]. The purified NPs were resuspended in phosphate-buffered saline (PBS) (1×) for further studies.

For the preparation of 50 mg of Ab-conjugated BEZ235 NPs, 50 mg of BEZ235 NPs (50 mg/ml) was incubated with 1 mg of DBCO-functionalized Ab (1 mg/ml) at 37°C for 1 hour. The Abs were quantitatively conjugated to the NPs.

The amount of encapsulated BEZ235 was quantified via fluorescence spectroscopy, as previously reported. Briefly, BEZ235 NPs (10 mg/ml) were digested with DMSO (nine times the volume of the NP dispersion) in the dark at 20°C for 24 hours. The concentration of BEZ235 was quantified in a fluorescence plate reader with excitation wavelength at 325 nm and emission wavelength at 425 nm. The amount of encapsulated BEZ235 was calculated by comparing the fluorescence intensities of drug-free NPs and standard BEZ235 solutions (in 1:9 PBS/DMSO). In vitro drug release study was performed via Slide-A-Lyzer MINI Dialysis Devices (20K MWCO, Thermo Fisher Scientific) at physiological conditions in the presence of a large excess of PBS (1×) at pH 7.0 or 6.0 (at 37°C in the dark). Unreleased BEZ235 was quantified spectroscopically, as previously reported.

Rhod NPs and Cy5 NPs were prepared via the same method except for 2.5% (w/w) of Rhod-labeled poly(lactide-*co*-glycolide) and Cy5-labeled poly(lactide) were added to the polymer blend before preparation of the NPs for in vitro and in vivo imaging studies.

Purified NPs were characterized by transmission electron microscopy (TEM) and NP tracking analysis (NTA) techniques. TEM images were recorded in a JEOL 1230 transmission electron microscope in Microscopy Services Laboratory (MSL) at the UNC School of Medicine. Before the imaging study, carbon-coated copper grids were glow discharged, and the samples were negatively stained with tungsten acetate (pH 7). NTA studies were performed in a NanoSight N500 (Malvern Panalytical Ltd.) instrument in the Nanomedicine Characterization Core Facility at the UNC Eshelman School of Pharmacy.

In vitro binding assay

In vitro binding was assessed via FACS method. Lymphoma cells were washed twice with azide-free FACS buffer and blocked with FACS buffer containing 5% FBS (for 30 min) before being stained with DBCO-functionalized Abs (for the pretargeted group) or Ab-conjugated Rhod NPs (for the active targeting group). In both experimental groups, 1×10^6 of lymphoma cells (in 100 μl of FACS buffer) were incubated with 1 μg of free or NP-anchored Ab. For the pretargeted group, cells were washed twice before being incubated with 60 μg of Rhod NPs at 37°C for 30 min. Stained cells were washed twice before being fixed with 10% neutral buffer formalin (NBF) for 5 min. For the active targeting groups, NP-stained cells were washed twice before fixing with 10% NBF for further study. In the control group, 1×10^6 of lymphoma cells were incubated with 60 μg of Rhod NPs at 37°C for 30 min. The cells were then washed twice and fixed before further analyses.

In vitro proliferation assay

The proliferation of different lymphoma cells after treatment with small-molecule ("free") BEZ235 and different active-targeted or pretargeted BEZ235 nanoformulations were assessed 72 hours after the initial treatment by CellTiter 96 AQueous Non-Radioactive Cell Proliferation Assay (Promega). Cells treated with free BEZ235 were washed once with complete medium 24 hours after the initial treatment to remove the free drug.

Western blots

Namalwa and Raji cells were treated with 500 nM free BEZ235 or different BEZ235 nanoformulations (via active targeted or pretargeted method) that contained 500 nM BEZ235 for 4 or 24 hours. Western blot samples were prepared as previously reported (*26*, *27*). Western blot studies were performed to quantify the p-AKT, AKT, p-S6, S6, and GAPDH expressions via an automated Western blot processor at RayBiotech Life (Georgia).

In vivo studies

Animals were maintained in the Division of Comparative Medicine [an Association for Assessment and Accreditation of Laboratory Animal Care International (AAALAC)–accredited experimental animal facility] under sterile environments at the UNC. All procedures involving experimental animals were performed in accordance with the protocols that the UNC Institutional Animal Care and Use Committee approved, and they conformed with the *Guide for the Care and Use of Laboratory Animals* (National Institutes of Health, publication no. 86-23, revised 1985).

In vivo NP uptake and biodistribution studies

In vivo NP uptake and biodistribution studies were performed in Raji xenograft tumor-bearing athymic nude mice [Crl:NU(NCr)-Foxn1^{nu}, origin: Charles River Laboratories]. Xenograft tumors were established by subcutaneous injection of 1×10^6 of Raji cells in 1:1 of RPMI 1640 medium and Matrigel to the left flank. Thirteen days after inoculation, mice received a single intraperitoneal injection of anti-NK1.1 Ab to deplete the natural killer (NK) cells. Fifteen days after inoculation, mice in different experimental groups were intravenously (tail vein) injected with different Cy5 NPs (5 mg of NPs per mouse). Mice in the pretargeting groups received a single intravenous injection of α-CD20(D), α-Lym1(D), or their 1:1 combination (total, 100 μg per mouse) of Abs 24 hours before the administration of the Cy5 NPs. Time-dependent epifluorescence images were recorded at different time points after injection of the Cy5 NPs using the AMI Optical Imaging System (Spectral Instruments Imaging Inc.; excitation, 605 ± 20 nm; emission, 690 ± 20 nm; exposure time, 30 s).

Mice were euthanized 48 hours after injection, and the xenograft tumor, full blood, and key organs were preserved and weighed for ex vivo imaging analyses in the AMI Optical Imaging System. The percentage of injected dose per gram (% ID/g) of tissue was calculated by comparing the photon counts versus standard Cy5 NPs.

In vivo antitumor activity study

The in vivo antitumor activity studies were performed in Namalwa and Raji xenograft tumor-bearing NSG mice (NOD.Cg-Prkdc^{scid} Il2rg^{tm1Wjl}/SzJ, female, origin: The Jackson Laboratory; 6 to 8 weeks old, 20 to 21 g). Xenograft tumors were established by subcutaneous injection of 1×10^6 cells in 1:1 of serum-free RPMI 1640 medium and Matrigel to the left flank. Mice received treatments 10 days after inoculation. The treatment doses were 100 μg of Ab and/or 50 μg of free/encapsulated BEZ235. A detailed treatment schedule and drug dosing are provided in the Supplementary Materials. Immunohistochemistry stains were performed on Raji xenograft tumors to evaluate the phospho–ribosomal protein S6 protein expression. Raji xenograft tumors (n = 4 per group) were preserved 48 hours after the first treatment for immunohistochemistry stains in the Translational Pathology Laboratory at the UNC School of Medicine.

In vivo toxicity study

An in vivo toxicity study was performed in healthy CD-1 mice [Crl:CD1(ICR), Charles River Laboratories; female, 10 to 11 weeks old, approximately 20 g]. Mice (5 per group) were intravenously administered with free BEZ235 [2.5 mg/kg; in 90:5:5 (v/v/v) of PBS/Cremophor EL/ethanol] or different BEZ235 nanoformulations that contained the same amount of encapsulated BEZ235 (i.e., 5 mg of BEZ235 NPs). In the pretargeting groups, 50 μg of α-CD20(D) plus 50 μg of α-Lym1(D) (or 50 μg of α-CD20 plus 50 μg of α-Lym1) were intravenously administered 24 hours before the BEZ235 NPs (or free BEZ235). Mice were euthanized via an overdose of ketamine 48 hours after the intravenous administration of different BEZ235 nanoformulations. Full blood and key organs were preserved for clinical chemistry and histopathological studies in the Animal Histopathology and Laboratory Medicine Core at the UNC School of Medicine.

SUPPLEMENTARY MATERIALS

Supplementary material for this article is available at http://advances.sciencemag.org/cgi/content/full/6/14/eaaz9798/DC1

View/request a protocol for this paper from *Bio-protocol*.

REFERENCES AND NOTES

1. R. L. Siegel, K. D. Miller, A. Jemal, Cancer statistics, 2019. *CA Cancer J. Clin.* **69**, 7–34 (2019).
2. B. Coiffier, C. Sarkozy, Diffuse large B-cell lymphoma: R-CHOP failure—What to do? *Hematology Am. Soc. Hematol. Educ. Program* **2016**, 366–378 (2016).
3. B. Coiffier, C. Thieblemont, E. Van Den Neste, G. Lepeu, I. Plantier, S. Castaigne, S. Lefort, G. Marit, M. Macro, C. Sebban, K. Belhadj, D. Bordessoule, C. Fermé, H. Tilly, Long-term outcome of patients in the LNH-98.5 trial, the first randomized study comparing rituximab-CHOP to standard CHOP chemotherapy in DLBCL patients: A study by the Groupe d'Etudes des Lymphomes de l'Adulte. *Blood* **116**, 2040–2045 (2010).
4. T. A. Davis, D. K. Czerwinski, R. Levy, Therapy of B-cell lymphoma with anti-CD20 antibodies can result in the loss of CD20 antigen expression. *Clin. Cancer Res.* **5**, 611–615 (1999).
5. P. Johnson, M. Glennie, The mechanisms of action of rituximab in the elimination of tumor cells. *Semin. Oncol.* **30**, 3–8 (2003).
6. P. McLaughlin, A. J. Grillo-López, B. K. Link, R. Levy, M. S. Czuczman, M. E. Williams, M. R. Heyman, I. Bence-Bruckler, C. A. White, F. Cabanillas, V. Jain, A. D. Ho, J. Lister, K. Wey, D. Shen, B. K. Dallaire, Rituximab chimeric anti-CD20 monoclonal antibody therapy for relapsed indolent lymphoma: Half of patients respond to a four-dose treatment program. *J. Clin. Oncol.* **16**, 2825–2833 (1998).
7. F. Naddafi, F. Davami, Anti-CD19 monoclonal antibodies: A new approach to lymphoma therapy. *Int. J. Mol. Cell Med.* **4**, 143–151 (2015).
8. J. P. Leonard, M. Coleman, J. C. Ketas, A. Chadburn, R. Furman, M. W. Schuster, E. J. Feldman, M. Ashe, S. J. Schuster, W. A. Wegener, H. J. Hansen, H. Ziccardi, M. Eschenberg, U. Gayko, S. Z. Fields, A. Cesano, D. M. Goldenberg, Epratuzumab, a humanized anti-CD22 antibody, in aggressive non-Hodgkin's lymphoma: Phase I/II clinical trial results. *Clin. Cancer Res.* **10**, 5327–5334 (2004).
9. A. L. Epstein, R. J. Marder, J. N. Winter, E. Stathopoulos, F. M. Chen, J. W. Parker, C. R. Taylor, Two new monoclonal antibodies, Lym-1 and Lym-2, reactive with human B-lymphocytes and derived tumors, with immunodiagnostic and immunotherapeutic potential. *Cancer Res.* **47**, 830–840 (1987).
10. L. A. Leslie, A. Younes, Antibody-drug conjugates in hematologic malignancies. *Am. Soc. Clin. Oncol. Educ. Book* 10.1200/EdBook_AM.2013.33.e108 (2013).
11. N. Diamantis, U. Banerji, Antibody-drug conjugates—An emerging class of cancer treatment. *Br. J. Cancer* **114**, 362–367 (2016).
12. M. Steiner, D. Neri, Antibody-radionuclide conjugates for cancer therapy: Historical considerations and new trends. *Clin. Cancer Res.* **17**, 6406–6416 (2011).
13. B. A. Teicher, R. V. Chari, Antibody conjugate therapeutics: Challenges and potential. *Clin. Cancer Res.* **17**, 6389–6397 (2011).
14. J. B. Haun, N. K. Devaraj, S. A. Hilderbrand, H. Lee, R. Weissleder, Bioorthogonal chemistry amplifies nanoparticle binding and enhances the sensitivity of cell detection. *Nat. Nanotechnol.* **5**, 660–665 (2010).
15. K. M. Au, A. Tripathy, C. P. Lin, K. Wagner, S. Hong, A. Z. Wang, S. I. Park, Bespoke pretargeted nanoradioimmunotherapy for the treatment of non-hodgkin lymphoma. *ACS Nano* **12**, 1544–1563 (2018).
16. J. A. Woyach, A. J. Johnson, J. C. Byrd, The B-cell receptor signaling pathway as a therapeutic target in CLL. *Blood* **120**, 1175–1184 (2012).
17. C. U. Niemann, A. Wiestner, B-cell receptor signaling as a driver of lymphoma development and evolution. *Semin. Cancer Biol.* **23**, 410–421 (2013).
18. K. Valla, C. R. Flowers, J. L. Koff, Targeting the B cell receptor pathway in non-Hodgkin lymphoma. *Expert Opin. Investig. Drugs* **27**, 513–522 (2018).
19. J. R. Westin, Status of PI3K/Akt/mTOR pathway inhibitors in lymphoma. *Clin. Lymphoma Myeloma Leuk.* **14**, 335–342 (2014).
20. C. L. Batlevi, A. Younes, Revival of PI3K inhibitors in non-Hodgkin's lymphoma. *Ann. Oncol.* **28**, 2047–2049 (2017).
21. E. Drakos, G. Z. Rassidakis, L. J. Medeiros, Mammalian target of rapamycin (mTOR) pathway signalling in lymphomas. *Expert Rev. Mol. Med.* **10**, e4 (2008).
22. J. S. Blachly, R. A. Baiocchi, Targeting PI3-kinase (PI3K), AKT and mTOR axis in lymphoma. *Br. J. Haematol.* **167**, 19–32 (2014).
23. F. Dituri, A. Mazzocca, G. Giannelli, S. Antonaci, PI3K functions in cancer progression, anticancer immunity and immune evasion by tumors. *Clin. Dev. Immunol.* **2011**, 947858 (2011).
24. K. Faia, K. White, E. Murphy, J. Proctor, M. Pink, N. Kosmider, K. M. Govern, J. Kutok, The phosphoinositide-3 kinase (PI3K)-δ,γ inhibitor, duvelisib shows preclinical synergy with multiple targeted therapies in hematologic malignancies. *PLOS ONE* **13**, e0200725 (2018).
25. S. M. O'Brien, N. Lamanna, T. J. Kipps, I. Flinn, A. D. Zelenetz, J. A. Burger, M. Keating, S. Mitra, L. Holes, A. S. Yu, D. M. Johnson, L. L. Miller, Y. Kim, R. D. Dansey, R. L. Dubowy, S. E. Coutre, A phase 2 study of idelalisib plus rituximab in treatment-naive older patients with chronic lymphocytic leukemia. *Blood* **126**, 2686–2694 (2015).
26. S. M. Maira, F. Stauffer, J. Brueggen, P. Furet, C. Schnell, C. Fritsch, S. Brachmann, P. Chène, A. De Pover, K. Schoemaker, D. Fabbro, D. Gabriel, M. Simonen, L. Murphy, P. Finan, W. Sellers, C. García-Echeverría, Identification and characterization of NVP-BEZ235, a new orally available dual phosphatidylinositol 3-kinase/mammalian target of rapamycin inhibitor with potent in vivo antitumor activity. *Mol. Cancer Ther.* **7**, 1851–1863 (2008).
27. J. Roper, M. P. Richardson, W. V. Wang, L. G. Richard, W. Chen, E. M. Coffee, M. J. Sinnamon, L. Lee, P.-C. Chen, R. T. Bronson, E. S. Martin, K. E. Hung, The dual PI3K/mTOR inhibitor NVP-BEZ235 induces tumor regression in a genetically engineered mouse model of PIK3CA wild-type colorectal cancer. *PLOS ONE* **6**, e25132 (2011).
28. C. Massard, K. N. Chi, D. Castellano, J. de Bono, G. Gravis, L. Dirix, J.-P. Machiels, A. Mita, B. Mellado, S. Turri, J. Maier, D. Csonka, A. Chakravartty, K. Fizazi, Phase Ib dose-finding study of abiraterone acetate plus buparlisib (BKM120) or dactolisib (BEZ235) in patients with castration-resistant prostate cancer. *Eur. J. Cancer* **76**, 36–44 (2017).
29. T. M. Wise-Draper, G. Moorthy, M. A. Salkeni, N. A. Karim, H. E. Thomas, C. A. Mercer, M. S. Beg, S. O'Gara, O. Olowokure, H. Fathallah, S. C. Kozma, G. Thomas, O. Rixe, P. Desai, J. C. Morris, A phase Ib study of the dual PI3K/mTOR inhibitor dactolisib (BEZ235) combined with everolimus in patients with advanced solid malignancies. *Target. Oncol.* **12**, 323–332 (2017).

30. S. Gholizadeh, J. A. A. M. Kamps, W. E. Hennink, R. J. Kok, PLGA-PEG nanoparticles for targeted delivery of the mTOR/PI3kinase inhibitor dactolisib to inflamed endothelium. *Int. J. Pharm.* **548**, 747–758 (2018).
31. L. Tian, Y. Qiao, P. Lee, L. Wang, A. Chang, S. Ravi, T. A. Rogers, L. Lu, B. Singhana, J. Zhao, M. P. Melancon, Antitumor efficacy of liposome-encapsulated NVP-BEZ 235 in combination with irreversible electroporation. *Drug Deliv.* **25**, 668–678 (2018).
32. R. R. Furman, J. P. Sharman, S. E. Coutre, B. D. Cheson, J. M. Pagel, P. Hillmen, J. C. Barrientos, A. D. Zelenetz, T. J. Kipps, I. Flinn, P. Ghia, H. Eradat, T. Ervin, N. Lamanna, B. Coiffier, A. R. Pettitt, S. Ma, S. Stilgenbauer, P. Cramer, M. Aiello, D. M. Johnson, L. L. Miller, D. Li, T. M. Jahn, R. D. Dansey, M. Hallek, S. M. O'Brien, Idelalisib and rituximab in relapsed chronic lymphocytic leukemia. *N. Engl. J. Med.* **370**, 997–1007 (2014).
33. G. Liu, A revisit to the pretargeting concept—A target conversion. *Front. Pharmacol.* **9**, 1476 (2018).
34. M. Patra, K. Zarschler, H.-J. Pietzsch, H. Stephan, G. Gasser, New insights into the pretargeting approach to image and treat tumours. *Chem. Soc. Rev.* **45**, 6415–6431 (2016).
35. F. Kraeber-Bodéré, C. Rousseau, C. Bodet-Milin, E. Frampas, A. Faivre-Chauvet, A. Rauscher, R. M. Sharkey, D. M. Goldenberg, J.-F. Chatal, J. Barbet, A pretargeting system for tumor PET imaging and radioimmunotherapy. *Front. Pharmacol.* **6**, 54 (2015).
36. F. Petronzelli, A. Pelliccia, A. M. Anastasi, V. D'Alessio, C. Albertoni, A. Rosi, B. Leoni, C. De Angelis, G. Paganelli, G. Palombo, M. Dani, P. Carminati, R. De Santis, Improved tumor targeting by combined use of two antitenascin antibodies. *Clin. Cancer Res.* **11**, 7137s–7145s (2005).
37. W. Poon, Y.-N. Zhang, B. Ouyang, B. R. Kingston, J. L. Y. Wu, S. Wilhelm, W. C. W. Chan, Elimination pathways of nanoparticles. *ACS Nano* **13**, 5785–5798 (2019).
38. J. M. Pagel, N. Orgun, D. K. Hamlin, D. S. Wilbur, T. A. Gooley, A. K. Gopal, S. I. Park, D. J. Green, Y. Lin, O. W. Press, A comparative analysis of conventional and pretargeted radioimmunotherapy of B-cell lymphomas by targeting CD20, CD22, and HLA-DR singly and in combinations. *Blood* **113**, 4903–4913 (2009).

Acknowledgments: We thank the Microscopy Service Laboratory Core, Animal Study Core, Small Animal Imaging Facility, Animal Clinical Laboratory, Animal Histopathology Core Facility, Translation Pathology Laboratory, UNC Flow Cytometry Core Facility, UNC Macromolecular Interactions Facility and UNC Michael Hooker Proteomics Center in the School of Medicine, and Chapel Hill Analytical and Nanofabrication Laboratory (CHANL) at the UNC at Chapel Hill for their assistance with procedures in this manuscript. The UNC Flow Cytometry Core Facility is supported, in part, by P30CA016086 Cancer Center Core Support Grant to the UNC Lineberger Comprehensive Cancer Center. **Funding:** This work was supported by the University Cancer Research Fund from the UNC and R01CA178748 grant from the NIH/National Cancer Institute. A.Z.W. was also supported by NIH Center for Nanotechnology Excellence grant U54-CA151652. S.I.P. was also supported by the American Cancer Society Mentored Research Scholar Grant in Tumor Biology and Genomics (126601-MRSG-14-215-01-TBG). **Author contributions:** K.M.A., S.I.P., and A.Z.W. conceived and designed the experiments. K.M.A. and the UNC Animal Study Core performed the experiments and analyzed data. K.M.A. and A.Z.W. cowrote the paper. All authors discussed the results and edited the manuscript at all stages. **Competing interests:** S.I.P. reports receiving research funding from Seattle Genetics, Teva, Takeda, and BMS; membership of speakers bureau for Gilead and Seattle Genetics; and membership on Board of Directors or advisory committee for Rafael Pharmaceuticals, BMS, and Teva. The authors declare that they have no other competing interests. **Data and materials availability:** All methods needed to evaluate the conclusions in the paper are present in the paper and/or the Supplementary Materials. All data related to this paper are available on request from the corresponding author.

Submitted 24 October 2019
Accepted 8 January 2020
Published 1 April 2020
10.1126/sciadv.aaz9798

Citation: K. M. Au, A. Z. Wang, S. I. Park, Pretargeted delivery of PI3K/mTOR small-molecule inhibitor–loaded nanoparticles for treatment of non-Hodgkin's lymphoma. *Sci. Adv.* **6**, eaaz9798 (2020).

ScienceAdvances

Pretargeted delivery of PI3K/mTOR small-molecule inhibitor–loaded nanoparticles for treatment of non-Hodgkin's lymphoma

Kin Man AuAndrew Z. WangSteven I. Park

Sci. Adv., 6 (14), eaaz9798. • DOI: 10.1126/sciadv.aaz9798

Science Advances (ISSN 2375-2548) is published by the American Association for the Advancement of Science. 1200 New York Avenue NW, Washington, DC 20005. The title *Science Advances* is a registered trademark of AAAS.